Corrosion Science xxx (xxxx) xxx–xxx

Contents lists available at ScienceDirect

Corrosion Science

journal homepage: www.elsevier.com/locate/corsci

Pyrophoric behaviour of ultrafine Mo powder

Lu Wang, Guo-Hua Zhang*, Shu-Qiang Jiao, Kuo-Chih Chou

State Key Laboratory of Advanced Metallurgy, University of Science and Technology Beijing, Beijing 100083, China

ARTICLE INFO

Keywords:
B. SEM
B. TEM
B. XPS
B. XRD
C. Oxidation
C. Passive films

ABSTRACT

The pyrophoric behaviour of as-reduced ultrafine Mo powder at 873 K was investigated. The dew point of the H_2 gas used in the preparation process had a significant effect on the pyrophoric behaviour of the resulting Mo powder as well as the product compositions. A low dew point of H_2 resulted in pyrophoric behaviour and the formation of γ-Mo_2N with a small amount of MoO_3 forming outside; in contrast, a high dew point of H_2 inhibited the pyrophoric behaviour. The morphology of the pyrophoric product was the same as that of the MoO_2 raw material.

1. Introduction

Molybdenum (Mo) possesses good high-temperature strength and creep resistance and a low coefficient of thermal expansion, which has led to its wide application as an alloying agent for manufacturing steel, cast iron, and superalloys [1,2]. Moreover, the use of ultrafine Mo powder with suitable morphology, size, and purity is critical for the fabrication of conductive films in electronic devices [3]. Nano-sized Mo powder is also recognized as possessing more attractive properties; therefore, its synthesis has been widely investigated in recent years.

Lamprey and Ripley [4] described a method for producing tungsten (W) and Mo metal powder with particle sizes of 0.01–0.1 μm via the hydrogen reduction of metal chlorides, Shibata et al. [5] prepared ultrafine metal Mo powder using the vapour phase reaction of the MoO_3-H_2 system, and Liu et al. [6] prepared nano-sized Mo powder using microwave plasma chemical vapour deposition. In addition, Nersisyan et al. [7] produced nano-structured Mo powder under self-propagating high-temperature synthesis mode (SHS) from the MoO_3-$NaBH_4$-*k*NaCl system (*k* is the mole number of NaCl), and Saghafi et al. [8] synthesized nanocrystalline Mo powder with a mean crystallite size of 50 nm by the mechanical activation of MoO_3 powder and its subsequent hydrogen reduction. In the authors' previous works [9–11], ultrafine Mo powder was successfully prepared by the hydrogen reduction of ultrafine MoO_2 powder, which was obtained by the hydrogen reduction of ultrafine spherical MoO_3.

Thus, many methods have been proposed to produce nano-sized or ultrafine Mo powder. However, during the preparation processes of nano-sized or ultrafine Mo powder, the as-prepared sample generally exhibits intensive pyrophoric behaviour when exposed to an air atmosphere even if the product is cooled to ambient temperature [4,12]. To date, there have been no reports in the literature on the pyrophoric behaviour of Mo powder or the corresponding phase transitions and morphology evolutions during the preparation process. The objective of the present work is to fill these gaps in the literature by investigating the factors affecting the pyrophoric properties of as-reduced ultrafine Mo powder. Our findings will be beneficial in selecting appropriate processing parameters to prevent the pyrophoric behaviour of as-prepared nano-sized or ultrafine Mo powder and improve the powder quality.

2. Materials and methods

2.1. Materials

Ultrafine MoO_2 powder prepared by hydrogen reduction of ultrafine spherical MoO_3 at 813 K was used as a raw material for the experiments [10]. Fig. 1 presents an X-ray diffraction pattern of the raw material; the peaks can be indexed as pure MoO_2 (PDF card No 32-671). The morphology of the raw material consisted of platelet-shaped particles with a fine particle size, as observed in Fig. 2.

2.2. Experimental procedure

Fig. 3 presents a schematic diagram of the experimental apparatus. High-purity Ar gas was further purified by passing through the molecular sieves (labelled'2') and colour-changing silica gels (labelled'3') (deoxidation and dehydration, respectively). The reducing gas H_2 was introduced via different routes (A–C), and the corresponding dew points of H_2 were 264 K (relative humidity: 9%, relative temperature: 298 K), 250. 9 K (relative humidity: 2.6%, relative temperature: 298 K),

* Corresponding author.
E-mail address: ghzhang_ustb@163.com (G.-H. Zhang).

http://dx.doi.org/10.1016/j.corsci.2017.09.006
Received 30 August 2017; Received in revised form 4 September 2017; Accepted 7 September 2017

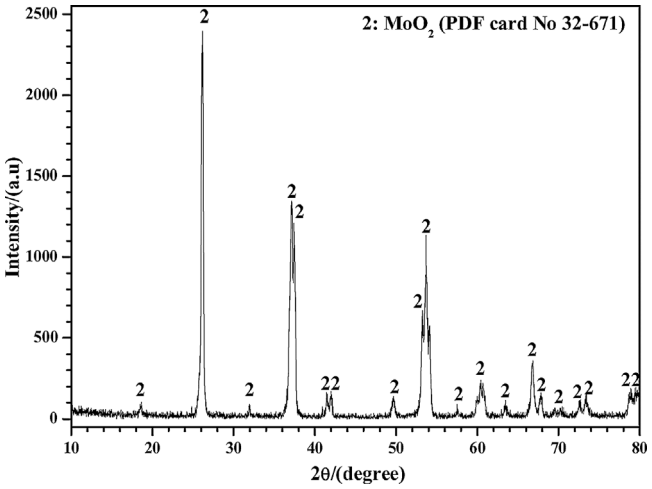

Fig. 1. XRD pattern of ultrafine MoO_2 powder (raw material).

and 273 K (relative humidity: 18.85%, relative temperature: 298 K), respectively. Once one of the routes was connected with port D, the remaining two switches were closed. For each route, approximately 100 mg MoO_2 samples were placed in an α-Al_2O_3 crucible (labelled '6') (ϕ 7 mm × 7 mm). After the crucible was placed into the quartz tube, Ar gas was introduced into the system to completely remove the air. Then, the quartz tube was placed into a Si-C electrical furnace at 873 K. When the temperature was stabilized, the Ar gas was switched to pure H_2 gas to start the reduction reaction. After reacting for a certain time, the reducing gas H_2 was switched to Ar gas again, and the quartz tube was rapidly removed to cool the samples to room temperature under the protection of Ar gas. Finally, the as-reduced samples were collected for examination.

The flow rates of both H_2 gas (< 5 ppm of O_2) and Ar gas (< 5 ppm of O_2) were maintained at 400 ml/min during the reduction and cooling processes for all the experiments. The prepared samples were characterized using X-ray diffraction (XRD; TTR III, Rigaku Corporation, Japan), field-emission scanning electron microscopy (FE-SEM; Zeiss SUPRA 55, Oberkochen, Germany), transmission electron microscopy (TEM) coupled with selected area electron diffraction (SAED) analysis (TECNAI G2 F30 S-TWIN, FEI Corporation, American), and X-ray photoelectron spectroscopy (XPS; ESCALAB 250 Xi, Thermo Scientific, American). The dew point of H_2 was measured using an intelligent dew point instrument (EN-7625, Shanghai Yingsheng Analysis Instrument Ltd., China).

3. Results

3.1. XRD analysis

After passing hydrogen through route A (without deoxidation and dehydration) and reacting for different times *t*, the products were examined using XRD, and the results are presented in Fig. 4. The XRD patterns reveal that in this case, MoO_2 was directly reduced to metal Mo without the formation of any intermediate oxides, as expected according to Eq. (1).

$$MoO_2 + 2H_2 = Mo + 2H_2O \quad (1)$$

In contrast, when hydrogen gas passed through route B (with deoxidation and dehydration) and reacted for different times *t*, the results greatly differed from those of route A. The corresponding XRD results are presented in Fig. 5. Surprisingly, if H_2 gas passed through route B, pure metal Mo powder was hardly obtained. Pure metal Mo was not obtained as the final reduction product even if the reduction time was prolonged to 300 min. In contrast, pure metal Mo was easily prepared after reduction for only 150 min using route A, as observed in Fig. 4. As observed in Fig. 5, four broad peaks were detected in all the XRD patterns for the product prepared using route B. These peaks were assigned to the γ-Mo_2N phase with face-centred cubic (fcc) crystal structure (PDF card No 25-1366). During the repeated experiments, the pure γ-Mo_2N phase was also sometimes obtained, as shown in Fig. 6. The signals at 37.44°, 43.52°, 63.14°, and 75.78°2θ (Cu Kα) were attributed to the (111), (200), (220), and (311) reflections, respectively. In addition, an obvious spark/flame was observed when the reaction products were removed from the quartz tube and exposed to the air atmosphere when the H_2 gas was introduced using route B, which indicated that the freshly prepared metal Mo powder under the current reduction condition exhibited an intense pyrophoric property. Thus, it can be deduced that MoO_2 was also first reduced to metal Mo, as shown in Eq. (1); once the as-prepared metal Mo was exposed to the air atmosphere, the pyrophoric reaction occurred to generate γ-Mo_2N, as indicated in Eq. (2).

$$4Mo + N_2 = 2Mo_2N \quad (2)$$

3.2. Morphological examination using FE-SEM

Fig. 7 presents FE-SEM micrographs of the reaction products obtained using route A (without deoxidation and dehydration). For the 50 min reaction time, the products almost had the same skeleton or dendritic structure as the MoO_2 raw material, as observed in Fig. 7(a) and (A). As the reaction continued (100 min), numerous cracks or fissures appeared, as observed in Fig. 7(b) and (B), which were created by the tensile stress generated from the volume decrease during the oxygen removal process [1,2,9,12]. When the reaction products were all metal Mo powder, as shown in Fig. 7(c) and (C), the products still retained the same platelet-shaped morphology as the MoO_2raw material. However, the as-obtained metal Mo powder had a higher porosity than the MoO_2 raw material.

However, when H_2 gas was introduced via route B (with deoxidation and dehydration), the morphology of the reduction products greatly differed from that using route A. The corresponding FE-SEM micrographs are presented in Fig. 8, which reveal that there was no obvious change in the morphology of the products as the reaction proceeded and the grain dimensions remained almost constant. Unlike the products prepared using route A in Fig. 7, the products prepared

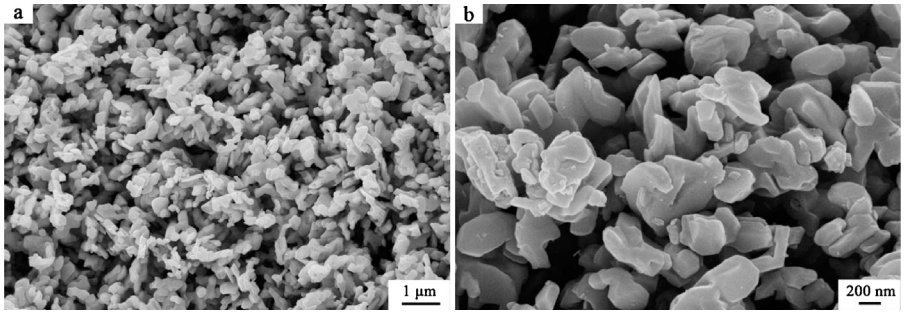

Fig. 2. Morphologies of ultrafine MoO_2 powder (raw material).